AGU ADVANCING EARTH AND SPACE SCIENCE

Geophysical Research Letters

RESEARCH LETTER
10.1029/2020GL088361

Key Points:
- We find an observed in-phase relationship between multidecadal North Atlantic SST variability and Florida summertime rainfall
- In climate models, runs with historical forcing are more likely to produce the observed relationship than control runs
- We add evidence that external forcing plays a meaningful role in the AMV with implications for future rainfall during Florida's flood season

Supporting Information:
- Supporting Information S1

Correspondence to:
J. M. Klavans,
jklavans@rsmas.miami.edu

Citation:
Klavans, J. M., Clement, A. C., Murphy, L. N., & Zhang, H. (2020). Identifying the externally forced Atlantic Multidecadal Variability signal through Florida rainfall. *Geophysical Research Letters*, *47*, e2020GL088361. https://doi.org/10.1029/2020GL088361

Received 9 APR 2020
Accepted 7 OCT 2020
Accepted article online 9 OCT 2020

Identifying the Externally Forced Atlantic Multidecadal Variability Signal Through Florida Rainfall

Jeremy M. Klavans[1], Amy C. Clement[1], Lisa N. Murphy[1], and Honghai Zhang[2]

[1]Rosenstiel School of Marine and Atmospheric Science, University of Miami, Miami, FL, USA, [2]Lamont-Doherty Earth Observatory, Columbia University, Palisades, NY, USA

Abstract The North Atlantic experiences basin-wide, multidecadal changes in sea surface temperature (SST), and this SST variability is linked with regional-to-continental scale impacts. These impacts often serve as motivation to study the underlying contributors to Atlantic Multidecadal Variability (AMV). However, these impacts can be more than motivation—they can be tools to study the AMV itself. Herein, we consider the positive correlation between Florida summertime rainfall and the AMV (Enfield et al., 2001, https://doi.org/10.1029/2000GL012745). First, we show that this relationship is apparent in updated observational data sets. Next, we demonstrate that large ensembles of climate models are capable of producing the observed relationship between the AMV and Florida summertime rainfall. Finally, using large ensembles from multiple climate models, we show that historical forcing makes models more likely to capture the observed relationship in summer precipitation. Our findings have implications for our understanding of the AMV and for precipitation projections in at-risk South Florida.

Plain Language Summary Ocean temperatures in the North Atlantic fluctuate from decade to decade. When the waters are warmer than average, we show that Florida gets more rain in late summer —at the same time as the region's highest high tides. Planning for the impacts of climate change on Florida requires that we understand the relationship between the temperature of the Atlantic Ocean and Florida precipitation. We show that changes in atmospheric composition (e.g., from greenhouse gases, pollution from industry, and ash and gases from volcanoes) make this connection more likely. So long as Atlantic Ocean temperatures continue to rise, we expect wetter late summer months in Florida in the future.

1. Introduction

Is there a role for climate impacts in causal studies of climate variability? Zhang et al.'s (2019) recent review of the ocean's contribution to Atlantic Multidecadal Variability (AMV) suggests that we consider a more "holistic" approach to evaluating potential causal mechanisms. Their review argues that decadal changes in the Atlantic Meridional Overturning Circulation (AMOC) cause basin-wide shifts in North Atlantic sea surface temperatures (SSTs; Zhang et al., 2019). This is a challenging causal case to make: Observational data are limited, and climate models may not adequately represent the AMOC and its variability (Buckley & Marshall, 2016; Danabasoglu et al., 2014; Kim et al., 2018). To augment limited direct observations, Zhang et al. (2019) consider a wide variety of AMOC covariates, such as tropical subsurface temperature, sea surface salinity, and heat fluxes. However, the relative contributions of ocean dynamics and external forcing to the AMV are still a subject of vigorous debate (e.g., Vecchi et al., 2017). In this paper, we extend Zhang et al.'s (2019) holistic approach to include local impacts and come to a parallel conclusion: There is a strong role for external forcing in the AMV.

Many previous studies argue that multidecadal North Atlantic SST variability is primarily a direct response to changes in external forcing (Bellomo et al., 2018; Bellucci et al., 2017; Birkel et al., 2018; Booth et al., 2012; Mann et al., 2020; Murphy et al., 2017; Otterå et al., 2010; Undorf et al., 2018; Watanabe & Tatebe, 2019). Climate models can produce the spatial pattern and timing of the AMV without the need for an interactive ocean (Clement et al., 2015; Murphy et al., 2017). The inclusion of greenhouse gases, anthropogenic aerosols, and volcanic aerosols in model runs all improve the simulated phasing of the AMV relative to observations (Bellomo et al., 2018). Periods of higher volcanic activity

are associated with both the early and middle twentieth century cool phases of the AMV (Birkel et al., 2018). Anthropogenic aerosols are also implicated in the post-1960 cool phase in observations and model experiments (Booth et al., 2012; Undorf et al., 2018; Watanabe & Tatebe, 2019). Of course, this line of thinking is not without criticism. For example, many of these studies rely on climate models, some of which may respond too strongly to external forcing (Kim et al., 2018; Zhang et al., 2013). The ability of a model to accurately capture forced variability is also limited by uncertainties in our estimates of historical forcing (Schmidt et al., 2011).

If the forced signal is a major component of the AMV, it ought to be detectable in local AMV impacts. One of the first AMV impacts to be documented is the in-phase relationship at decadal time scales between North Atlantic SSTs and boreal summer Florida precipitation (Enfield et al., 2001; Mestas-Nūnez & Enfield, 2003; Obeysekera et al., 2007; Ruprich-Robert et al., 2018). Florida summertime precipitation is partitioned into an early and late rainy season by an intervening midsummer drought (Martinez et al., 2019). These subseasonal features are caused by the balance between the movement of regional-scale atmospheric circulation features and the extent of the Western Hemisphere Warm Pool (WHWP; Martinez et al., 2019; Mestas-Nūnez & Enfield, 2003). The onset of the early rainy season (May–June) is characterized by the northward migration of the Intertropical Convergence Zone (ITCZ) and the expansion of the western edge of the North Atlantic Subtropical High (NASH; Martinez et al., 2019). During the midsummer drought (July–August) the NASH continues expanding westward limiting moisture transport into the region. In the late rainy season (September–October), as the NASH recedes into the Atlantic and the ITCZ shifts southward, the WHWP reaches its spatial zenith allowing for enhanced moisture convergence across Florida and the Caribbean (Martinez et al., 2019; Wang & Enfield, 2001). Because of the waning dynamical control from NASH and the waxing thermodynamical impacts from WHWP, the late rainy season precipitation is thermodynamically tied to tropical Atlantic SSTs and the AMV (Sutton & Hodson, 2005, 2007). In fact, Li et al. (2010) show that on multidecadal time scales during the late rainy season, observed NASH intensity and western extent are not statistically significantly correlated with the AMV. These results corroborate that the multidecadal changes in Florida summertime rainfall are predominately a thermodynamic response to the AMV.

Late rainy season decadal Florida rainfall is a good testbed for the forced signal in the AMV because any forced changes in SST should be thermodynamically coupled to precipitation without invoking noisier dynamical responses. More concisely, there should be a high signal-to-noise ratio in Florida rainfall. Late rainy season precipitation is of particular importance to Floridians. Annual perigean spring tides or "king tides" generally occur in October and cause the largest "sunny day floods." Local governments are already in the process of spending millions of dollars to mitigate the influence of sea level rise, with many additional billions of dollars expected to be needed (e.g., Harris, 2019). Projecting changes in precipitation that will coincide with these floods is vital to planners working to adapt to sea level rise.

We do not expect to find a large externally forced signal in Florida rainfall in climate models either (1) during the dry season or (2) when the AMV signal is transmitted via underresolved or unresolved processes. During the dry season the signal from internal variability in the tropical Pacific Ocean, described by El Niño–Southern Oscillation (ENSO) indices, is the largest interannual control on Florida rainfall (Enfield et al., 2001; Kushnir et al., 2010; Trenberth et al., 1998). As this pattern is internally generated, we expect that it will average out across many runs of a single climate model. Externally forced signals will also be difficult to detect if and when the AMV is connected to Florida precipitation via processes reliant on high spatial or temporal resolution. Known processes observationally linked to the AMV include the number of Atlantic hurricanes and precipitation extremes (Curtis, 2008; Goldenberg et al., 2001; Goly & Teegavarapu, 2014; Teegavarapu et al., 2013).

Using an ensemble of large ensembles, we show that historical forcing makes models more likely to capture the observed relationship between the AMV and Florida late rainy season precipitation. In section 2, we describe the utility of the ensemble of large ensembles approach as well as the data and methods employed in this analysis. In section 3 we extend and describe the observed relationship between Florida summertime rainfall and evaluate that relationship in an ensemble of climate model ensembles. We conclude by discussing the role of forcing in the AMV and ponder how forced precipitation variability may affect coastal Florida during their flooding season.

2. Methods and Data

2.1. Ensemble of Large Ensembles

Understanding the relative roles of internal variability and external forcing in producing the AMV closely mirrors so-called "detection and attribution" studies that attempt to isolate the anthropogenic influence on climate variables (Bindoff et al., 2013). Large ensembles of climate models isolate a forced response by sampling over the range of internal variability that is produced by a given model, then averaging it out (Kay et al., 2015). Independent time histories of internal variability are produced via either minute perturbations in initial conditions or with changes to the state of the ocean (Hawkins et al., 2016). Using an ensemble of large ensembles allows us to sample over structural uncertainty associated with single models (Deser et al., 2020).

We use output from six different ensembles collected in the Multi-Model Large Ensemble Archive (MMLEA; Deser et al., 2020; Jeffrey et al., 2013; Kay et al., 2015; Kirchmeier-Young et al., 2017; Maher et al., 2019; Rodgers et al., 2015; Sun et al., 2018). Supporting information Table S1 lists information about each ensemble considered herein. All ensembles are run at a relatively coarse resolution to study local rainfall. Although the magnitude of monthly average rainfall is lower in the models compared to observations, a clear seasonal cycle is still visible (Figure S1). Our analysis considers different starting years for each model simulation (1850, 1920, or 1950) through Model Year 2020. All models are forced with estimates of historical forcing through 2005 and with scenario-based estimates of external forcing through 2020 (Meinshausen et al., 2011). For parsimony, we call these runs "historically forced" as the differences between observed forcing and scenario forcing between 2005 and 2020 are minor (Peters et al., 2013). All models use Representative Concentration Pathway (RCP) 8.5, except MPI-ESM-LR, which uses a combination of RCP8.5, RCP4.5, and RCP2.6. All three scenarios have similar emissions trajectories and atmospheric carbon dioxide concentrations for the years we consider, 2006–2020 (Meinshausen et al., 2011). We exclude EC-Earth because precipitation output was not available in the MMLEA.

For each model that is part of the MMLEA, we also consider a companion long preindustrial (PI) control run. In these runs, external forcing is held constant. Comparison between PI control runs and the MMLEA allows us to experimentally isolate the role of historical forcing. To make direct comparisons between each model in the MMLEA and their corresponding PI control run, we create a 10,000-member synthetic PI ensemble, via bootstrap, where the block size is equal to the length of the corresponding ensemble's historically forced run (see Table S1).

2.2. Observational Data Sets

We rely on three precipitation products to test the relationship between the AMV and Florida rainfall. For our map and Florida state-wide averages we use a 1° × 1° configuration of the Global Precipitation Climatology Project version 2018 (GPCP) gridded monthly precipitation product covering the years 1901–2016 (Schneider et al., 2014). To allow for direct comparison to Enfield et al. (2001), we consider a selection from NOAA's Disk Resident Database (DRD964x or DRD) divisional precipitation data set that covers the years 1895–2013 (Guttman & Quayle, 1996). We also consider the updated NOAA nClimDiv divisional precipitation product for the years 1895–2017 (Vose et al., 2014). For both of the NOAA data sets we consider Florida climate divisions one through five, which span from the Florida panhandle (division one) through the peninsula (divisions two to five) but exclude the Florida Keys and the South Florida coastline (see Figure S2). We also consider data from WMO rain gauges with 60-year-long records or greater that are part of NOAA's Climate Anomaly Monitoring System accessed through the IRI/LDEO Data Library: 72202 (Miami), 72203 (Palm Beach), 72205 (Orlando), 72206 (Jacksonville), 72211 (Tampa), 72214 (Tallahassee), and 72222(Pensacola).

For observed SST, we use the Extended Reconstructed Sea Surface Temperature Version 5 (ERSSTv5) (Huang et al., 2017). ERSSTv5 extends from 1854 to the present; however, we use subsections that match the length of the precipitation records cited above.

For our analysis of Florida landfalling hurricanes, we use the International Best Track Archive for Climate Stewardship version 4 (IBTrACS; Knapp et al., 2010). IBTrACS extends from 1851 to 2019. In this paper, we use the years 1854–2017 to allow for comparison with our precipitation products. We only consider landfalling Florida hurricanes, which should limit our exposure to some presatellite biases in the data set.

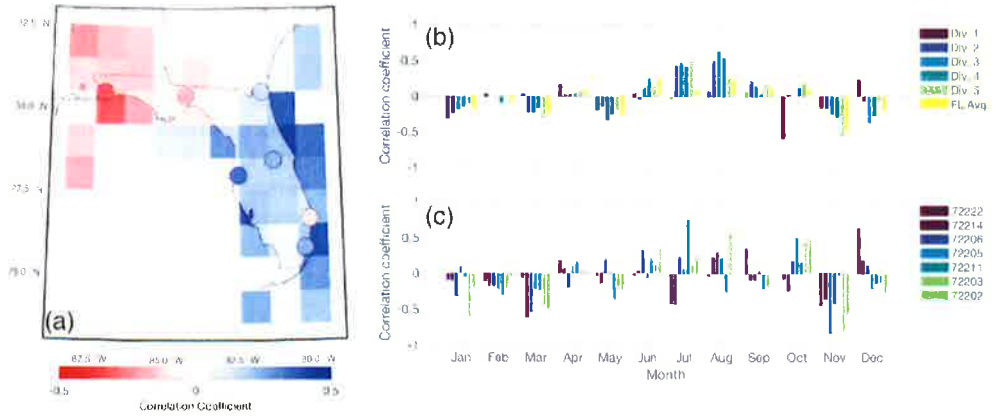

Figure 1. Relationship between the observed AMV and observed Florida precipitation in June–October. (a) Colors show the correlation with the observed AMV and GPCP. Filled circles show the correlation with individual rain gauges. (b) Monthly correlations of the AMV with nClimDiv and our GPCP Florida average precipitation index (yellow). (c) Correlation of the AMV index with individual rain gauges. Bar colors represent the NOAA climate division from Panel (b) the gauges lie in.

However, particularly early in the record, there is still uncertainty over landfall location and the completeness of the archive.

2.3. Indices

We calculate the AMV index by first finding the area-weighted average SST between 0–60°N and 80°W to 0°E for the given month/season/year. We then linearly detrend this time series and low-pass filter with a Lanczos filter using a 1/10-year half-power frequency. We linearly detrend to remove the linear SST response to greenhouse gas forcing while retaining the influence of time-varying forced signals (e.g., aerosols and volcanic eruptions; Murphy et al., 2017).

Florida average precipitation from GPCP and the MMLEA is calculated as the area-weighted average precipitation over Florida peninsular land (25–28°N, 88–80°W). For model runs, ensemble mean indices are calculated by first averaging the entire field of monthly output from all ensemble members, then creating the appropriate index. All fields and indices are low-pass filtered unless otherwise noted.

3. Results

3.1. Observations

In observations, there is a positive and significant correlation between the AMV and decadal Florida rainy season precipitation (June–October; JJASO). This was alluded to in Enfield et al. (2001), who qualitatively note that the annual average pattern of the multidecadal precipitation response to the AMV over the United States was dominated by the summertime signal. Similarly, other recent work implies a strong summertime signal via their choice of study season (e.g., Curtis, 2008; Goly & Teegavarapu, 2014). In JJASO, for both DRD and nClimDiv, we find positive and significant correlations for climate divisions two through five, regardless of the choice of study period (Table S2). The correlation between the AMV and our GPCP index (JJASO) is 0.31 (95% CI: 0.14–0.46). We note that in GPCP there is a larger correlation (r = 0.56, 95% CI: 0.41–0.67) when we only use data through 1999. Given the difference in correlations between study periods is only statistically significant in one climate division (division three; Table S2), we speculate that any differences are likely due to internal variability. Figure 1a illustrates the pattern of precipitation associated with the AMV across Florida in gridded data and in rain gauges. Overall, results are similar to the regional indices reported above. The negative correlation observed in the Florida panhandle and the Pensacola station (72202) is consistent with the drying signal in the rest of the southeastern United States during the warm phase of the AMV (Kushnir et al., 2010; Sutton & Hodson, 2005, 2007; Watanabe & Tatebe, 2019).

Within Florida's rainy season, the strongest observed signal appears at the end of the midsummer drought and the beginning of the late rainy season. Figure 1b shows that in peninsular Florida (divisions two through five), there is a strong and positive relationship in July and August. Across these four divisions, the nClimDiv average correlation for July and August are 0.36 and 0.40, respectively. Conversely, the average correlation for the other 10 months is −0.08. Although noisier, we find a similar positive relationship between the peninsular rain gauges and the AMV (Figure 1c).

In the data sets and time periods we consider, we cannot conclusively identify statistically significant relationship between annual average Florida rainfall and the AMV. When we evaluate the same precipitation data set as Enfield et al. (2001; DRD) against our SST data set (ERSST), we do not identify a positive and statistically significant correlation between the AMV and annual average precipitation (divisions one through five; Table S3). This is true for either the 1895–1999 period (as in Enfield et al., 2001) or our updated 1895–2013 period. However, in NOAA's newer nClimDiv product we do find a positive and significant correlation between the AMV and annual average precipitation in divisions three through five for the period 1895–1999 (Table S3). The significant correlations in nClimDiv hold in only divisions four and five when we include data through 2016 (Table S2). In an index of Florida peninsular rainfall constructed from GPCP, we do not find a statistically meaningful relationship, in the annual average (for data ending in 1999, $r = 0.06$, 95% CI: −0.13–0.24, and for data ending in 2016, $r = -0.08$, 95% CI: −0.25–0.10). None of the rain gauges that we consider show a statistically significant correlation between the AMV and rainfall in the annual average. When including additional years of observations and additional data sets, we cannot conclusively confirm the annual average result from Enfield et al. (2001). However, given the strong summer signal discussed above, much of their interpretation is useful for understanding Florida rainfall.

Although it is not the focus of this study, we note that during the winter dry season the AMV is associated with a small, negative precipitation anomaly. This is consistent with Goly and Teegavarapu's (2014) results examining precipitation extremes. Of course, the Florida dry season precipitation is known to have a stronger connection to the ENSO (Sutton & Hodson, 2007). To avoid confounding this known mode of internal variability's dynamical influence on Florida precipitation and potential influences of forcing on ENSO (e.g., DiNezio et al., 2009), we exclude the dry season from the model analysis in section 3.2.

On multidecadal time scales, there is not enough evidence to make a statistical link between the AMV index and the history of Florida landfalling hurricanes. Between 1854 and 2017, we identify 93 storms that make landfall in Florida as a hurricane. The limited sample size associated with these extreme events hinders our ability to draw statistically valid conclusions. There is a small and positive correlation between the annual average AMV index and the number of landfalling hurricanes in Florida ($r = 0.18$, 95% CI: 0.02–0.32). This is expected given the well-known relationship between SST, cyclogenesis (Emanuel, 2003), and vertical shear (Goldenberg et al., 2001). Filtering to look for a low-frequency relationship reduces the degrees of freedom and does not yield a statistically significant relationship. We cannot confirm or exclude the possibility that the AMV-Florida rainfall relationship is moderated by changes in the number of landfalling hurricanes.

3.2. Models

Individual ensemble members of historically forced runs and synthetic ensemble members of PI control runs can produce positive relationships between the AMV and Florida rainfall (Figure 2a). In JJASO, positive correlations are more likely to occur in historically forced ensembles than in the PI synthetic ensembles: 68% of MMLEA ensemble members produce a positive correlation compared to 50% of PI synthetic ensemble members. However, precipitation is a noisy field. The distribution of correlations from MMLEA is not statistically significantly distinguishable from 0 for any model in any month. So historical forcing makes a faithful reproduction of the observed positive correlation more likely but does not guarantee that an individual ensemble member will reproduce the relationship.

The forced (or ensemble mean) relationship between the AMV and Florida rainfall in the late rainy season is almost always positive, as in observations. Across all six MMLEA models for JJASO, 26 out of 30 historically forced ensemble mean correlations are positive (87%). That is, the relationship between the forced portion of the AMV and the forced portion of Florida precipitation is nearly always positive over JJASO. Runs without historical forcing do not consistently produce positive relationships. Only 50% of the "ensemble means" from the PI ensemble are positive over JJASO, as would be expected if the two processes were independent

Figure 2. The relationship between the AMV and Florida rainfall in the MMLEA. (a) Box-and-whisker plots show the ensemble spread in correlations from each ensemble in each month (boxes: 25th to 75th percentile ensemble member). The filled dot shows the ensemble mean. Gray blocks represent the "ensemble" spread (calculated via bootstrap) from the corresponding PI control run. (b) The probability that the forced response has a higher correlation than any ensemble member for each ensemble in each month. (c) The monthly average SST in the WHWP for each model and for observations (ERSSTv5; 1854–2019). Colored box and whiskers are historically forced runs; vertically aligned gray crosses are PI control runs.

(not shown). Likewise, the average MMLEA JJASO ensemble mean correlation is 0.46, while the average synthetic PI "ensemble mean" correlation is −0.01. Within the rainy season, the largest positive correlations in the MMLEA occur in the late rainy season, when Florida rainfall is thermodynamically tied to SSTs (Figure 2a). The in-phase relationship between the AMV and Florida rainfall in the ensemble mean pulls the entire ensemble toward the observed, positive correlation. With historical forcing, MMLEA models are more likely to faithfully reproduce the observed correlation in JJASO.

Could these large historically forced correlations be due to chance? Figure 2b charts the probability that the ensemble mean has a larger correlation than all of the individual ensemble members. That is, where does the ensemble mean correlation intersect the empirical cumulative distribution function calculated from the correlations from individual ensemble members? These values can help us determine how likely it is that internal variability within a model is capable of producing a forced relationship that large and positive (1 minus the values in Figure 2b). As above, the highest likelihood for the forced signal to be outside of the ensemble spread is in the late rainy season. By the same metric for the PI synthetic ensemble, we find no relationship between seasonality and the probability of a positive ensemble mean. Overall, we find that historical forcing makes reproducing this AMV impact more likely and this is unlikely to be due to chance.

4. Discussion

We show that historical forcing makes models more likely to faithfully reproduce a known AMV impact. We extend the analysis in Enfield et al. (2001) and show that there is a positive, statistically significant relationship between the observed AMV and Florida rainfall in late summertime using rain gauges and precipitation products. In large ensembles of multiple climate models, the inclusion of historical forcing makes models more likely to recover the observed in-phase relationship between Florida rainfall and the AMV. Previous work shows that including estimates of historical forcing allows climate models to better reproduce the

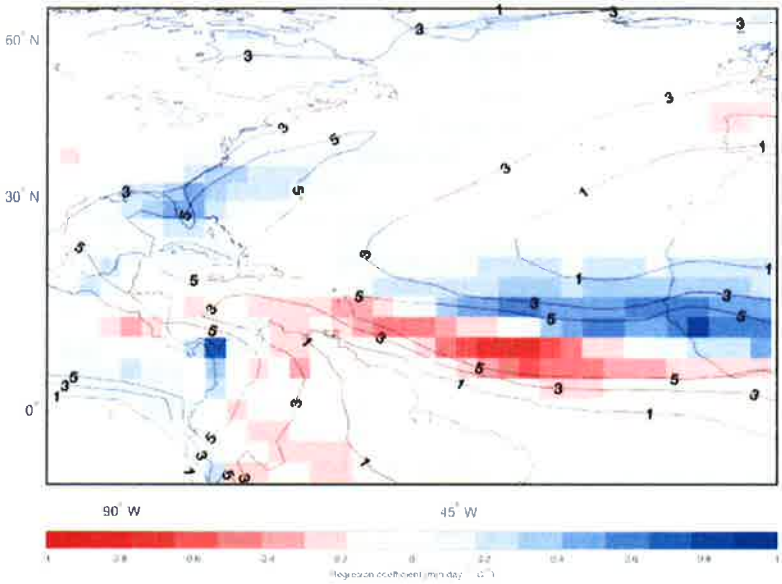

Figure 3. The multimodel mean September–October forced precipitation response to the forced AMV (colors) overlaid by the multimodel mean climatological September–October precipitation (contours; mm day^{-1}). Pixel-wise regressions were calculated between the ensemble mean AMV and the ensemble mean precipitation for each model individually. Models were averaged with equal weights. We only include those regression coefficients that are statistically significant at the 95% level.

phasing of the observed AMV index (Bellomo et al., 2018; Booth et al., 2012; Murphy et al., 2017; Undorf et al., 2018; Watanabe & Tatebe, 2019). Here we show that historical forcing also makes models more likely to reproduce a significant AMV impact in this region.

In the MMLEA, enhanced late summertime precipitation is a thermodynamic response to the externally forced AMV (Martinez et al., 2019). In all six models, a local spatial precipitation maximum develops over Florida in September–October. This pattern of precipitation appears to be amplified by the warmer SSTs associated with the positive phase of the AMV. That is, the forced precipitation response to the AMV coincides with the late summer precipitation mean state near Florida (Figure 3). This proposed explanation is consistent with Held and Soden's (2006) thermodynamically driven "wet-get-wetter" mechanism. Further, it pairs well with more recent studies that show that wet seasons may get wetter with changes in external forcing (e.g., Chou et al., 2013; Konapala et al., 2020). We hypothesize that the Florida rainfall-AMV signal is stronger in historically forced models than in PI control runs because there is no consistent atmospheric circulation response (as viewed through sea level pressure) to the AMV that can interrupt the thermodynamic relationship between the AMV and precipitation (compare right-hand sides of Figures S3 and S4).

Additionally, we find that warmer mean Atlantic SSTs generally improve the model's ability to produce our relationship of interest. For example, CESM has a known cold bias in the tropical Atlantic, potentially related to the structure of AMOC, and has a cooler WHWP in JJASO than all other MMLEA models (Figure 2c; Wang et al., 2014; Zhang et al., 2019). These cooler mean SSTs may account for the weaker forced signal in CESM relative to other MMLEA models (Figure 2). This is consistent with the Held and Soden (2006) mechanism; warmer Atlantic SSTs help amplify the Florida rainfall response to the AMV. Additionally, CESM may suffer from a potential circulation bias, wherein on average the western edge of the NASH lingers over Florida later into the year than other models (Figure S5).

In the future, mean Atlantic SSTs will continue to warm with anthropogenic forcing, which ought to lead to a stronger signal in the AMV-Florida rainfall relationship. When we exclude the more anthropogenically forced years 2006–2020 from our analysis, we find a weaker (but still positive) relationship. As noted above, when we remove historical forcing completely (as in PI control runs) the AMV and Florida rainfall appear to

be independent. This implies that including at least some of the forced response in the definition of the AMV is useful for understanding AMV impacts.

The results above also demonstrate the utility of the ensemble of large ensembles approach (Deser et al., 2020). For example, CESM-LENS produces a weaker relationship between the AMV and Florida late summertime rainfall than other MMLEA models. If we had only studied this ensemble, we may have reached a spurious conclusion about the nature of the AMV. However, in the context of additional models, we find that the results from CESM are potentially related to multiple model biases.

Prior studies have shown the warm phase of the AMV increases Florida precipitation in the wet season through changes in extremes (Goly & Teegavarapu, 2014; Teegavarapu et al., 2013). In Florida, a statistically significant portion of extreme precipitation events is linked to hurricanes (Barlow, 2011; Kunkel et al., 2010). Tropical cyclone precipitation rates are expected to change with external forcing (Knutson et al., 2020). Here we do not statistically confirm or exclude landfalling hurricanes as the mechanism linking the AMV and precipitation anomalies in observations. However, given the links between the AMV, external forcing, hurricanes, and Florida precipitation, we believe that causal studies of these phenomena in climate models will be a fruitful avenue of future research.

Finally, coastal Florida experiences their king tides during the late rainy season, when models suggest the largest forced signal in multidecadal Florida precipitation. As seas rise with global mean temperature, the frequency and duration of coastal floods are expected to increase (Sweet et al., 2017). In the near term, if the AMV index continues its warming trend, we expect that late summer months in Florida will get wetter in the future.

Data Availability Statement

GPCPv7 and NOAA ERSSTv5 data are provided by NOAA/OAR/ESRL PSD (https://www.esrl.noaa.gov/psd/). DRD, nClimDiv, and IBTrACS data are provided by NOAA (https://ncdc.noaa.gov). Rain gauge data were downloaded from the IRI/LDEO data library (https://iridl.ldeo.columbia.edu/). Access and download to the MMLEA was facilitated by NCAR's supercomputing resources provided by NSF/CISL/Cheyenne (see http://www.cesm.ucar.edu/projects/community-projects/MMLEA/).

Acknowledgments
We acknowledge grants from the NSF Climate and Large-Scale Dynamics program and the NSF Paleo Perspectives on Climate Change program.

References

Barlow, M. (2011). Influence of hurricane-related activity on North American extreme precipitation. *Geophysical Research Letters, 38*, L04705. https://doi.org/10.1029/2010GL046258

Bellomo, K., Murphy, L. N., Cane, M. A., Clement, A. C., & Polvani, L. M. (2018). Historical forcings as main drivers of the Atlantic Multidecadal Variability in the CESM large ensemble. *Climate Dynamics, 50*(9-10), 3687–3698. https://doi.org/10.1007/s00382-017-3834-3

Bellucci, A., Mariotti, A., & Gualdi, S. (2017). The role of forcings in the twentieth-century North Atlantic Multidecadal Variability: The 1940–75 North Atlantic Cooling Case Study. *Journal of Climate, 30*(18), 7317–7337. https://doi.org/10.1175/JCLI-D-16-0301.1

Bindoff, N. L., Stott, P. A., AchutaRao, K. M., Allen, M. R., Gillett, N., Gutzler, D., et al. (2013). Detection and attribution of climate change: From global to regional. In T. F. Stocker et al. (Eds.), *Climate change 2013: The physical science basis. Contribution of Working Group I to the Fifth Assessment Report of the Intergovernmental Panel on Climate Change* (pp. 867–952). Cambridge: Cambridge University Press.

Birkel, S. D., Mayewski, P. A., Maasch, K. A., Kurbatov, A. V., & Lyon, B. (2018). Evidence for a volcanic underpinning of the Atlantic Multidecadal Oscillation. *npj Climate and Atmospheric Science, 1*(1), 1, 24–7. https://doi.org/10.1038/s41612-018-0036-6

Booth, B. B. B., Dunstone, N. J., Halloran, P. R., Andrews, T., & Bellouin, N. (2012). Aerosols implicated as a prime driver of twentieth-century North Atlantic climate variability. *Nature, 484*(7393), 228–232. https://doi.org/10.1038/nature10946

Buckley, M. W., & Marshall, J. (2016). Observations, inferences, and mechanisms of the Atlantic Meridional Overturning Circulation: A review. *Reviews of Geophysics, 54*, 5–63. https://doi.org/10.1002/2015RG000493

Chou, C., Chiang, J. C. H., Lan, C.-W., Chung, C.-H., Liao, Y.-C., & Lee, C.-J. (2013). Increase in the range between wet and dry season precipitation. *Nature Geoscience, 6*(4), 263–267. https://doi.org/10.1038/ngeo1744

Clement, A., Bellomo, K., Murphy, L. N., Cane, M. A., Mauritsen, T., Rädel, G., & Stevens, B. (2015). The Atlantic Multidecadal Oscillation without a role for ocean circulation. *Science, 350*(6258), 320–324. https://doi.org/10.1126/science.aab3980

Curtis, S. (2008). The Atlantic Multidecadal Oscillation and extreme daily precipitation over the US and Mexico during the hurricane season. *Climate Dynamics, 30*(4), 343–351. https://doi.org/10.1007/s00382-007-0295-0

Danabasoglu, G., Yeager, S. G., Bailey, D., Behrens, E., Bentsen, M., Bi, D., et al. (2014). North Atlantic simulations in Coordinated Ocean-Ice Reference Experiments Phase II (CORE-II). Part I: Mean states. *Ocean Modelling, 73*, 76–107. https://doi.org/10.1016/j.ocemod.2013.10.005

Deser, C., Lehner, F., Rodgers, K. B., Ault, T., Delworth, T. L., DiNezio, P. N., et al. (2020). Insights from Earth system model initial-condition large ensembles and future prospects. *Nature Climate Change, 10*(4), 277–286. https://doi.org/10.1038/s41558-020-0731-2

DiNezio, P. N., Clement, A. C., Vecchi, G. A., Soden, B. J., Kirtman, B. P., & Lee, S.-K. (2009). Climate response of the equatorial Pacific to global warming. *Journal of Climate, 22*(18), 4873–4892. https://doi.org/10.1175/2009JCLI2982.1

Emanuel, K. (2003). Tropical cyclones. *Annual Review of Earth and Planetary Sciences, 31*(1), 75–104. https://doi.org/10.1146/annurev.earth.31.100901.141259

Enfield, D. B., Mestas-Nuñez, A. M., & Trimble, P. J. (2001). The Atlantic Multidecadal Oscillation and its relation to rainfall and river flows in the continental U.S. *Geophysical Research Letters, 28*(10), 2077–2080. https://doi.org/10.1029/2000GL012745

Goldenberg, S. B., Landsea, C. W., Mestas-Nuñez, A. M., & Gray, W. M. (2001). The recent increase in Atlantic hurricane activity: Causes and implications. *Science, 293*(5529), 474–479. https://doi.org/10.1126/science.1060040

Goly, A., & Teegavarapu, R. S. V. (2014). Individual and coupled influences of AMO and ENSO on regional precipitation characteristics and extremes. *Water Resources Research, 50*, 4686–4709. https://doi.org/10.1002/2013WR014540

Guttman, N. B., & Quayle, R. G. (1996). A historical perspective of U.S. climate divisions. *Bulletin of the American Meteorological Society, 77*(2), 293–303. https://doi.org/10.1175/1520-0477(1996)077<0293:AHPOUC>2.0.CO;2

Harris, A. (2019). A $3 billion problem: Miami-Dade's septic tanks are already failing due to sea rise. Miami Herald. https://www.miamiherald.com/news/local/environment/article224132115.html

Hawkins, E., Smith, R. S., Gregory, J. M., & Stainforth, D. A. (2016). Irreducible uncertainty in near-term climate projections. *Climate Dynamics, 46*(11-12), 3807–3819. https://doi.org/10.1007/s00382-015-2806-8

Held, I. M., & Soden, B. J. (2006). Robust responses of the hydrological cycle to global warming. *Journal of Climate, 19*(21), 5686–5699. https://doi.org/10.1175/JCLI3990.1

Huang, B., Thorne, P. W., Banzon, V. F., Boyer, T., Chepurin, G., Lawrimore, J. H., et al. (2017). Extended Reconstructed Sea Surface Temperature, Version 5 (ERSSTv5): Upgrades, validations, and intercomparisons. *Journal of Climate, 30*(20), 8179–8205. https://doi.org/10.1175/JCLI-D-16-0836.1

Jeffrey, S., Rotstayn, L., Collier, M., Dravitzki, S., Hamalainen, C., Moeseneder, C., et al. (2013). Australia's CMIP5 submission using the CSIRO Mk3. 6 model. *Australian Meteorological and Oceanographic Journal, 63*(1), 1–14. https://doi.org/10.22499/2.6301.001

Kay, J. E., Deser, C., Phillips, A., Mai, A., Hannay, C., Strand, G., et al. (2015). The Community Earth System Model (CESM) large ensemble project: A community resource for studying climate change in the presence of internal climate variability. *Bulletin of the American Meteorological Society, 96*(8), 1333–1349. https://doi.org/10.1175/BAMS-D-13-00255.1

Kim, W. M., Yeager, S., Chang, P., & Danabasoglu, G. (2018). Low-frequency North Atlantic climate variability in the Community Earth System Model large ensemble. *Journal of Climate, 31*(2), 787–813. https://doi.org/10.1175/JCLI-D-17-0193.1

Kirchmeier-Young, M. C., Zwiers, F. W., & Gillett, N. P. (2017). Attribution of extreme events in Arctic sea ice extent. *Journal of Climate, 30*(2), 553–571. https://doi.org/10.1175/JCLI-D-16-0412.1

Knapp, K. R., Kruk, M. C., Levinson, D. H., Diamond, H. J., & Neumann, C. J. (2010). The International Best Track Archive for Climate Stewardship (IBTrACS). *Bulletin of the American Meteorological Society, 91*(3), 363–376. https://doi.org/10.1175/2009BAMS2755.1

Knutson, T., Camargo, S. J., Chan, J. C. L., Emanuel, K., Ho, C.-H., Kossin, J., Mohapatra, M., et al. (2020). Tropical cyclones and climate change assessment: Part II: Projected response to anthropogenic warming. *Bulletin of the American Meteorological Society, 101*(3), E303–E322. https://doi.org/10.1175/BAMS-D-18-0194.1

Konapala, G., Mishra, A. K., Wada, Y., & Mann, M. E. (2020). Climate change will affect global water availability through compounding changes in seasonal precipitation and evaporation. *Nature Communications, 11*(1), 3044. https://doi.org/10.1038/s41467-020-16757-w

Kunkel, K. E., Easterling, D. R., Kristovich, D. A. R., Gleason, B., Stoecker, L., & Smith, R. (2010). Recent increases in U.S. heavy precipitation associated with tropical cyclones. *Geophysical Research Letters, 37*, L24706. https://doi.org/10.1029/2010GL045164

Kushnir, Y., Seager, R., Ting, M., Naik, N., & Nakamura, J. (2010). Mechanisms of tropical Atlantic SST influence on North American precipitation variability. *Journal of Climate, 23*(21), 5610–5628. https://doi.org/10.1175/2010JCLI3172.1

Li, W., Li, L., Rong, F., Deng, Y., & Wang, H. (2010). Changes to the North Atlantic subtropical high and its role in the intensification of summer rainfall variability in the southeastern United States. *Journal of Climate, 24*(5), 1499–1506. https://doi.org/10.1175/2010JCLI3829.1

Maher, N., Milinski, S., Suarez-Gutierrez, L., Botzet, M., Dobrynin, M., Kornblueh, L., et al. (2019). The Max Planck Institute grand ensemble: Enabling the exploration of climate system variability. *Journal of Advances in Modeling Earth Systems, 11*, 2050–2069. https://doi.org/10.1029/2019MS001639

Mann, M. E., Steinman, B. A., & Miller, S. K. (2020). Absence of internal multidecadal and interdecadal oscillations in climate model simulations. *Nature Communications, 11*(1), 49–49. https://doi.org/10.1038/s41467-019-13823-w

Martinez, C., Goddard, L., Kushnir, Y., & Ting, M. (2019). Seasonal climatology and dynamical mechanisms of rainfall in the Caribbean. *Climate Dynamics, 53*(1-2), 825–846. https://doi.org/10.1007/s00382-019-04616-4

Meinshausen, M., Smith, S. J., Calvin, K., Daniel, J. S., Kainuma, M. L. T., Lamarque, J. F., et al. (2011). The RCP greenhouse gas concentrations and their extensions from 1765 to 2300. *Climatic Change, 109*, 1(1-2), 213–241. https://doi.org/10.1007/s10584-011-0156-z

Mestas-Nûnez, A. M. & Enfield, D. B. (2003). Investigation of intra-seasonal to multi-decadal variability in South Florida rainfall.

Murphy, L. N., Bellomo, K., Cane, M., & Clement, A. (2017). The role of historical forcings in simulating the observed Atlantic Multidecadal Oscillation. *Geophysical Research Letters, 44*, 2472–2480. https://doi.org/10.1002/2016GL071337

Obeysekera, J., Trimble, P., Neidrauer, C., & Cadavid, L. (2007). Consideration of climate variability in water resources planning and operations—South Florida's experience. In *World Environmental and Water Resources Congress 2007: Restoring Our Natural Habitat*, 1–11.

Otterå, O. H., Bentsen, M., Drange, H., & Suo, L. (2010). External forcing as a metronome for Atlantic Multidecadal Variability. *Nature Geoscience, 3*(10), 688–694. https://doi.org/10.1038/ngeo955

Peters, G. P., Andrew, R. M., Boden, T., Canadell, J. G., Ciais, P., Le Quéré, C., et al. (2013). The challenge to keep global warming below 2°C. *Nature Climate Change, 3*(1), 4–6. https://doi.org/10.1038/nclimate1783

Rodgers, K. B., Lin, J., & Frölicher, T. L. (2015). Emergence of multiple ocean ecosystem drivers in a large ensemble suite with an earth system model. *Biogeosciences, 12*(11), 3301–3320. https://doi.org/10.3929/ethz-b-000101963

Ruprich-Robert, Y., Delworth, T., Msadek, R., Castruccio, F., Yeager, S., & Danabasoglu, G. (2018). Impacts of the Atlantic Multidecadal Variability on North American summer climate and heat waves. *Journal of Climate, 31*(9), 3679–3700. https://doi.org/10.1175/JCLI-D-17-0270.1

Schmidt, G. A., Jungclaus, J. H., Ammann, C. M., Bard, E., Braconnot, P., Crowley, T. J., et al. (2011). Climate forcing reconstructions for use in PMIP simulations of the last millennium (v1. 0). *Geoscientific Model Development, 4*(1), 33–45. https://doi.org/10.5194/gmd-4-33-2011

Schneider, U., Becker, A., Finger, P., Meyer-Christoffer, A., Ziese, M., & Rudolf, B. (2014). GPCC's new land surface precipitation climatology based on quality-controlled in situ data and its role in quantifying the global water cycle. *Theoretical and Applied Climatology, 115*(1–2), 15–40. https://doi.org/10.1007/s00704-013-0860-x

Sun, L., Alexander, M., & Deser, C. (2018). Evolution of the global coupled climate response to Arctic sea ice loss during 1990–2090 and its contribution to climate change. *Journal of Climate*, *31*(19), 7823–7843. https://doi.org/10.1175/JCLI-D-18-0134.1

Sutton, R. T., & Hodson, D. L. R. (2005). Atlantic Ocean forcing of North American and European summer climate. *Science*, *309*(5731), 115–118. https://doi.org/10.1126/science.1109496

Sutton, R. T., & Hodson, D. L. R. (2007). Climate response to basin-scale warming and cooling of the North Atlantic Ocean. *Journal of Climate*, *20*(5), 891–907. https://doi.org/10.1175/JCLI4038.1

Sweet, W. V., Kopp, R. E., Weaver, C. P., Obeysekera, J., Horton, R. M., Thieler, E. R., & Zervas, C. (2017). Global and regional sea level rise scenarios for the United States. NOAA Technical Report NOS CO-OPS 083. NOAA/NOS Center for Operational Oceanographic Products and Services.

Teegavarapu, R. S. V., Goly, A., & Obeysekera, J. (2013). Influences of Atlantic Multidecadal Oscillation phases on spatial and temporal variability of regional precipitation extremes. *Journal of Hydrology*, *495*, 74–93. https://doi.org/10.1016/j.jhydrol.2013.05.003

Trenberth, K. E., Branstator, G. W., Karoly, D., Kumar, A., Lau, N.-C., & Ropelewski, C. (1998). Progress during TOGA in understanding and modeling global teleconnections associated with tropical sea surface temperatures. *Journal of Geophysical Research*, *103*(C7), 14,291–14,324. https://doi.org/10.1029/97JC01444

Undorf, S., Bollasina, M. A., Booth, B. B. B., & Hegerl, G. C. (2018). Contrasting the effects of the 1850–1975 increase in sulphate aerosols from North America and Europe on the Atlantic in the CESM. *Geophysical Research Letters*, *45*, 11,930–11,940. https://doi.org/10.1029/2018GL079970

Vecchi, G. A., Delworth, T. L., & Booth, B. (2017). Climate science: Origins of Atlantic decadal swings. *Nature*, *548*(7667), 284–285. https://doi.org/10.1038/nature23538

Vose, R. S., Applequist, S., Squires, M., Durre, I., Menne, M. J., Williams, C. N., et al. (2014). Improved historical temperature and precipitation time series for U.S. climate divisions. *Journal of Applied Meteorology and Climatology*, *53*(5), 1232–1251. https://doi.org/10.1175/JAMC-D-13-0248.1

Wang, C., & Enfield, D. B. (2001). The tropical Western Hemisphere Warm Pool. *Geophysical Research Letters*, *28*(8), 1635–1638. https://doi.org/10.1029/2000GL011763

Wang, C., Zhang, L., Lee, S.-K., Wu, L., & Mechoso, C. R. (2014). A global perspective on CMIP5 climate model biases. *Nature Climate Change*, *4*(3), 201–205. https://doi.org/10.1038/nclimate2118

Watanabe, M., & Tatebe, H. (2019). Reconciling roles of sulphate aerosol forcing and internal variability in Atlantic multidecadal climate changes. *Climate Dynamics*, *53*(7–8), 4651–4665. https://doi.org/10.1007/s00382-019-04811-3

Zhang, R., Delworth, T. L., Sutton, R., Hodson, D. L. R., Dixon, K. W., Held, I. M., et al. (2013). Have aerosols caused the observed Atlantic multidecadal variability?. *Journal of the Atmospheric Sciences*, *70*(4), 1135–1144. https://doi.org/10.1175/jas-d-12-0331.1

Zhang, R., Sutton, R., Danabasoglu, G., Kwon, Y.-O., Marsh, R., Yeager, S. G., et al. (2019). A review of the role of the Atlantic Meridional Overturning Circulation in Atlantic Multidecadal Variability and associated climate impacts. *Reviews of Geophysics*, *57*, 316–375. https://doi.org/10.1029/2019RG000644